Proceedings of the 6th JFPS International
Symposium on Fluid Power, TSUKUBA 2005
November 7-10, 2005

EXPLICIT FINITE ELEMENT ANALYSIS OF TRACKING CAPABILITY OF ROTARY FACE SEAL FOR INDUSTRIAL FLUID POWER APPLICATIONS

Olof CALONIUS and Matti PIETOLA

Department of Mechanical Engineering
Helsinki University of Technology
P.O. Box 4400, FI-02015 TKK, Finland
(E-mail: Olof.Calonius@tkk.fi)

ABSTRACT

Seals are generally inexpensive machine elements, but in industrial fluid power systems the costs of sealing failure can be much higher than the cost of replacing the damaged seal due to, e.g., costs related to process downtime. Consequently, careful design evaluation is needed. In this study, the capability of a large diameter rotary face seal of spring-loaded type to respond to unwanted axial motion between the sealing surfaces caused by sudden changes in loading of components of the process machinery was evaluated.
Explicit finite element analysis, well suited for highly non-linear problems involving frictional contact, was used to compute the response of the seal to forced relative axial motion of the sealing surfaces. For condition monitoring, temporal variation of the total contact force exerted on the counterface, i.e., the sealing force during excitations was recorded, representing simple virtual sensor output describing the relation between axial motion and contact situation.

KEY WORDS

Explicit, Finite, Element, Face, Seal

NOMENCLATURE

B	:	Seal cross-section width [mm]
b	:	Spring cross-section width [mm]
E	:	Young's modulus [N/m^2]
H	:	Seal cross-section height [mm]
h	:	Spring cross-section height [mm]
$PTFE$	:	Polytetrafluoroethylene
R	:	Seal contact radius [mm]
r	:	Radial coordinate [mm]
t	:	Spring thickness [mm]
W	:	Seal contact width [mm]
α	:	Coefficient of thermal expansion [1/°C]
μ	:	Friction coefficient [-]
ν	:	Poisson's ratio [-]
ω	:	Angular velocity [1/s]
ρ	:	Density [kg/m^3]
σ_Y	:	Yield stress [N/m^2]

INTRODUCTION

This study was motivated by a need to evaluate prospective seal designs of critical components in process machinery. In a previous study [1], an initial seal profile shape of two different sizes was investigated in which the seal lip had approximately the same radial location as the actuation zone of the spring. For this study, the seal profile was modified by changing the radial location of the lip in relation to the actuation zone of the spring in order to increase the contact pressure on

the oil side of the lip. The capability of the modified rotary face seal design to react to excessive axial motion between the sealing surfaces was investigated. In addition, for condition monitoring purposes, the contact situation between the seal and the counterface was monitored by recording the sealing force values during axial motion excitations.

METHODS

Seal model

The cross-section of the seal is shown in Figure 1. The dimensions were R = 249 mm, W = 0.2 mm, B = 13 mm, H = 7 mm, b = 6 mm, h = 4 mm and t = 0.26 mm. A corresponding axisymmetric finite element model of the seal was built, Figure 2. Abaqus/Explicit was used for solving the response to the axial excitations. The model comprised 450 CAX4R elements in the seal jacket and 168 CAX4R elements in the spring. The rotor, clamp and counterface were modeled as rigid parts.

Frictional contact was specified between the different parts. In the static joints between seal and clamp and seal and rotor the coefficient of friction was 0.1. The same value was chosen for the dynamic joint between seal and counterface because relatively high contact stresses were expected at the seal lip and sliding speed in the radial direction was expected to be low [2]. For the seal-spring contact pair three different friction coefficient values were tested: μ = 0.06, 0.18, 0.36. The base value of 0.06 was chosen to represent friction between seal and spring at low sliding speeds [3]. The other values were chosen to model the effect that dirt and deposits could have on the dynamic behavior of the seal-spring contact.

Temperature dependent properties for the glass fiber filled *PTFE* material of the seal jacket [4] and the Hastelloy C-22 [5] spring were chosen according to Table 1. A Drucker-Prager material model was chosen for the *PTFE* material in Abaqus to be able to model the fact that the material had higher yield stress in compression than in tension. The same model was previously used in [1], in which the dependence between stress and plastic strain also was listed.

Analysis steps and loads

The actual analyses consisted of determining the response of the seal to relative motion between the rotor and the counterface. To be able to study the response, computations to obtain the operating conditions were conducted. The seal was first clamped against the rotor and subsequently compressed 0.9 mm against the counterface. Then the operating temperature distribution, the rotational body force and the pressure load were applied. The analyses were therefore carried out as four consecutive computational steps: 1) clamp, 2) compress, 3) apply operating conditions and 4) apply excitation.

The analysis time was 0.05 s in the three first steps and 2.05 s in the excitation step, 2.20 s in total. To speed up the analyses in Abaqus/Explicit, mass scaling was used [6]; scaling factor 100 in steps 1)–3) and 400 in step 4).

The temperature distribution in the seal profile was computed in a separate heat transfer analysis in Abaqus/standard. This was a simplified analysis in that only temperature boundary conditions corresponding to typical design requirements were applied. The temperatures in the response analyses varied from 100 °C at the contact zone of the seal lip to 60 °C in regions in contact with the oil and 40 °C in boundary regions elsewhere. The centrifugal effects were taken into account by applying a rotational body force ($\rho r \omega^2$, ω = 81.7 1/s) in the radial direction to the spring and the seal jacket. The parts of the seal jacket in contact with the oil were loaded with a pressure of 0.05 MPa.

Excitations

Forced displacement excitations were applied to the seal-clamp-rotor combination to produce relative motion between the seal and the counterface. During the excitations the rotor and the clamp were allowed to move only in the axial direction and the seal and the spring interacted with the other parts only through frictional contact.

Two different excitations were applied. Excitation 1 was produced from measurements of the relative motion between rotor and counterface in an industrial setting during a change in the loading of the machinery, Figure 3 (a). The displacement signals were obtained by twice integrating the output signals of accelerometers measuring motion in the axial direction. The relative motion signal was produced by filtering (band-pass 0.5-6 Hz) the displacement signals and computing their difference. This filtered relative motion signal is shown in Figure 3 (b) together with Excitation 2, a sinusoidal signal with an amplitude of 0.6 mm representing a situation of unwanted excessive relative motion.

RESULTS

Sealing force

The sealing force, i.e., the temporal variation of the total contact force exerted by the seal on the counterface, recorded the response to different excitations. Abnormal contact situations, loss of contact or excessive contact outside the seal lip, were easily detected, as shown in Figure 4 (a). During Excitation 1 the maximum, minimum and average values of the sealing force were 3.3 kN, 0.86 kN and 1.95 kN, respectively. These values were computed for μ = 0.06 between seal and spring. The influence of seal-spring friction on the seal dynamics was found to be small as shown in Figure 4 (b). For all three values of μ tested, nearly the same force response was obtained.

Stresses and contact pressure

The contour plot in Figure 5 shows the axial stresses in the seal cross-section during normal operation (seal in base position after compression).

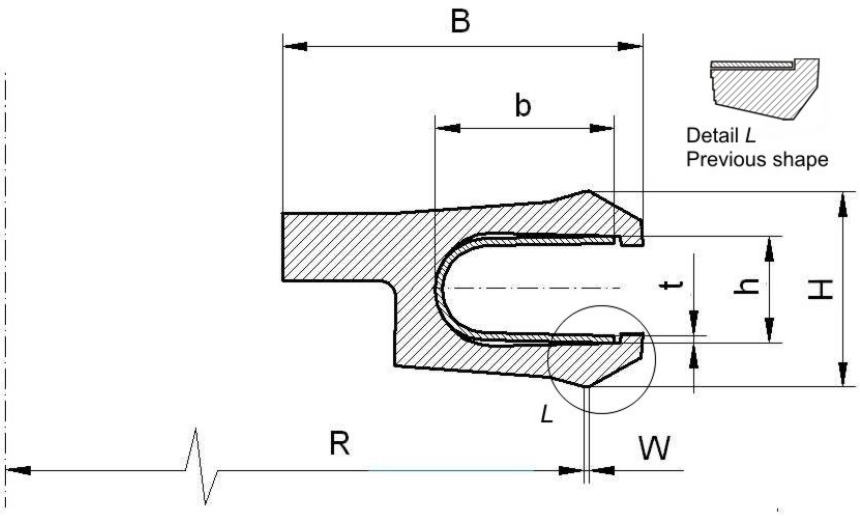

Figure 1 Cross-section of seal. Oil space on the right and air space on the left, towards the rotation axis. Dynamic sealing zone (*W*) will be in contact with the counterface. Upper parts of seal will be clamped against rotor. Detail *L* shows earlier seal lip design.

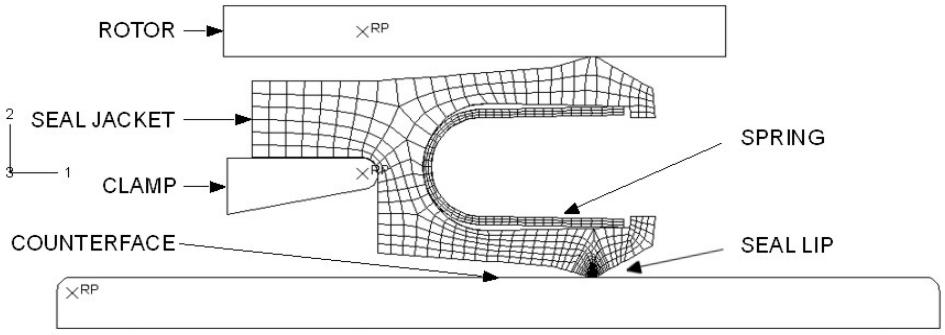

Figure 2 Finite element model of spring-loaded face seal. Configuration before clamping and precompression shown. Axial direction is vertical and radial direction is to the right.

Table 1 Material properties

Property	*PTFE*	Hastelloy
σ_Y	6 MPa @ 23 °C 1.8 MPa @ 120 °C	408 MPa @ 24 °C 373 MPa @ 93 °C
E	600 MPa @ 23 °C 205 MPa @ 120 °C	206 GPa @ 24 °C 203 GPa @ 93 °C
ν	0.46	0.3
ρ	2160 kg/m^3	8690 kg/m^3
α	1.9×10^{-4} 1/°C (1)	1.1×10^{-5} 1/°C

(1) For temperatures above 31 °C (3.3×10^{-4} 1/°C in range 19-31 °C)

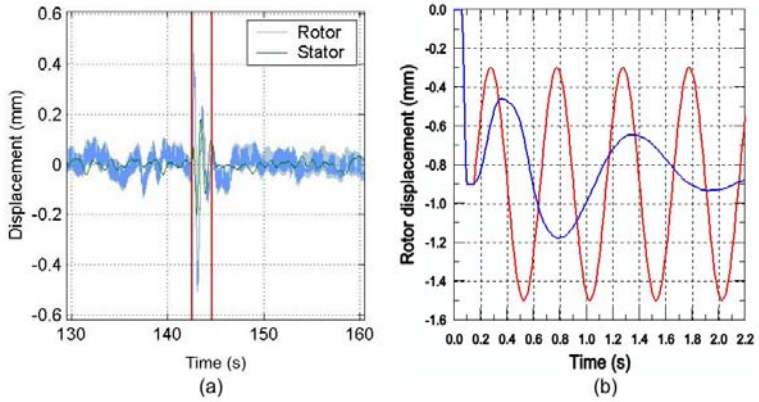

Figure 3 (a) Measured motion of rotor and counterface (stator) in process machinery. Change of loading at approximately 142 s. Excitation 1 has been produced from signals between vertical lines. (b) Excitations applied to the seal-clamp-rotor combination. Curve in middle is Excitation 1, produced from the filtered signals in (a). Sinusoidal curve is Excitation 2, an artificial motion signal used for studying the effects of excessive motion and diagnostic capability of the virtual total contact force sensor.

As a result of clamping, there were high compressive stresses, reaching −10 MPa, in the seal flange. At the end of Excitation 1 there were high tensile/compressive bending stresses in the spring (+284 / −315 MPa) and in the vertical part of the seal profile (+4.6 / −4.7 MPa). In the beginning of the excitation the highest stresses in the spring exceeded the yield stress. Yielding was restricted to few elements close to the symmetry line of the spring in the outer element layers.

Figure 5 also shows the stress field resulting from excessive contact between the vertical part of the seal and the counterface. A collision of this kind leads to permanent deformation of the profile with large plastic strains developing in the middle of the vertical part of the seal profile where there already were high compressive stresses during normal operation. In this region the axial compressive stresses reached −14 MPa and the equivalent plastic strains reached 7%. High axial compressive stresses were present in the seal lip at the contact zone. At the end of Excitation 1 the maximum compressive stress reached approximately −10 MPa. At the same time there were substantial radial compressive stresses in the seal lip reaching −5.6 MPa. High bending stresses also developed in the lower part of the seal between the vertical part and the lip. During Excitation 1 the highest values were ± 9 MPa.

Figure 6 shows close-ups of the seal lip of both an earlier design and the current design. The axial stress concentration due to contact was on the air side of the contact zone. The contact pressure distribution under the seal lip was roughly parabolic in shape, Figure 7. When the seal profile was in base position (corresponding to 0.9 mm compression) the contact pressure dropped to zero at the nodes closest to the oil side.

DISCUSSION

Current seal lip design

The current seal lip design was conceived under the hypothesis that by moving the seal contact zone somewhat towards the air side, the spring would exert more pressure on the oil side of the contact zone compared to the earlier design, c.f. Figure 6. A design in which the peak of the contact pressure distribution is located on the oil side is often considered a prerequisite for good sealing capability in lip seals [7–9]. It appears, see Figures 6 and 7, that the design change was not radical enough. The peak of the contact pressure distribution did not relocate to the oil side of the sealing zone. The lower part of the seal jacket still pivots about the air side edge of the seal lip during axial motion.

Apart from the high stresses in the seal flange caused by clamping, there were three high stress regions. High bending stresses were found in the vertical part of the seal, next to the clamp, and in the horizontal part between the vertical part and the seal lip. During Excitation 1 plastic strains developed in the latter region. In the seal lip, near the contact zone, the compressive stresses clearly exceeded the yield stress.

Tracking capability

The tracking capability of the current seal was found to be adequate for coping with the measured axial motion (Excitation 1) produced by changes in loading of the machinery. However, as shown by the response of the seal to Excitation 2 (Figures 4 and 5), small changes in the motion amplitude can cause leakage or even damage the seal, if it is not protected against excessive compression by proper seal housing design.

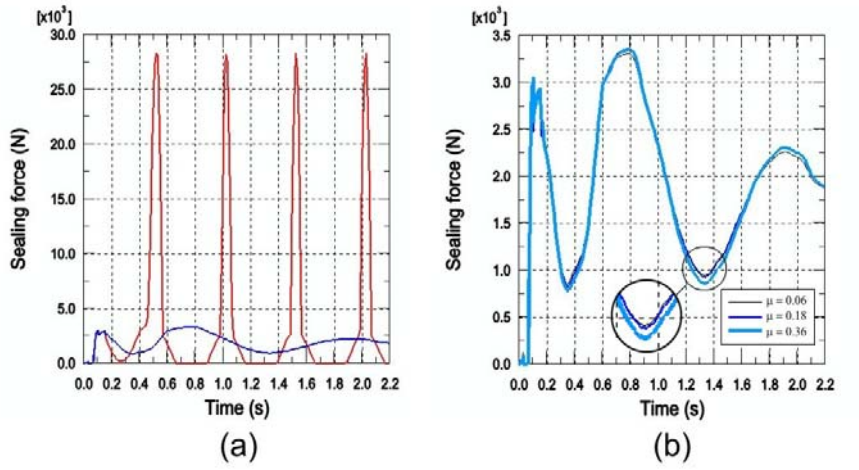

Figure 4 (a) Sealing force values corresponding to Excitation 1 (smoother curve) and to Excitation 2 (curve with spikes). Zero sealing force indicates loss of contact, while spikes indicate contact outside intended contact zone.
(b) Effect of friction between seal and spring (μ = 0.06, 0.18 and 0.36) on sealing force for Excitation 1. In the figure, the line width increases with the value of μ.

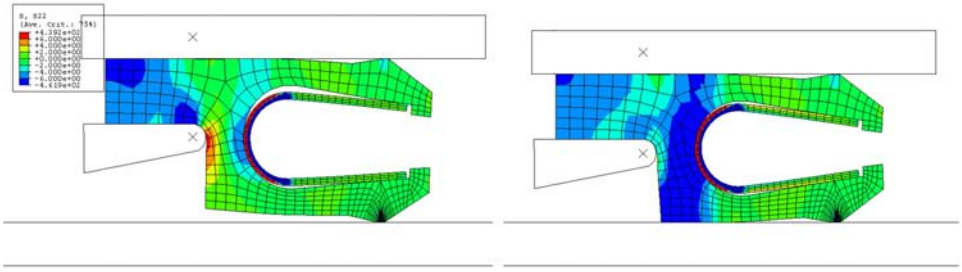

Figure 5 Vertical, i.e., axial stresses in seal profile. Seal in base position after compression shown left and vertical part of seal colliding with counterface due to excessive axial motion (Excitation 2) shown right. High compressive stresses are produced in the attachment flange and typical bending stresses are seen in vertical regions of seal and spring. The collision results in high compressive stresses in the vertical part of the seal and deformation of the profile.

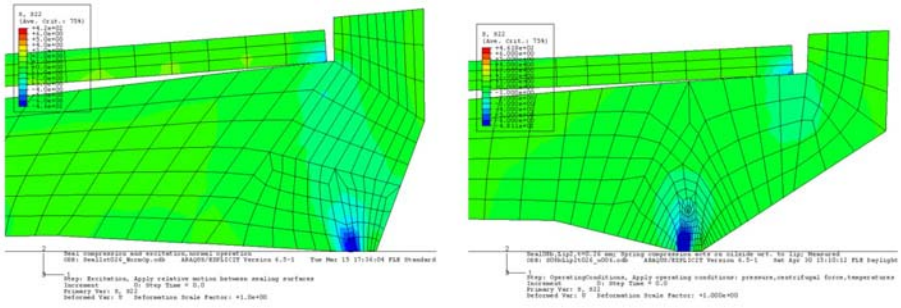

Figure 6 Vertical stresses in seal lip. Earlier lip shape shown left and current lip shape shown right. In both cases the highest compressive stresses are located towards the air side of the contact zone.

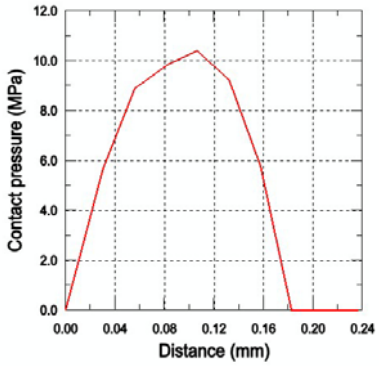

Figure 7 Contact pressure distribution under seal lip for current seal design. Seal profile in base position after Excitation 1.

Note that the seal maintains contact (non-zero sealing force) with the counterface during the first cycle of Excitation 2, Figure 4 (a). It is only after the collision that loss of contact occurs during the recession part of the motion cycle. As long as the seal is undamaged, a natural upper limit on the rebound travel is the precompression, 0.9 mm in this case [1].

For the axisymmetric model the sealing force appeared to be a simple but appropriate indicator describing the overall contact situation between seal and counterface. A similar indicator was the temporal variation of the internal energy (strain energy plus plastic dissipation). For example, the internal energy curve had spikes coinciding with situations of excessive contact, but the sealing force curve depicts this situation more clearly. Loss of contact can also be more easily discerned from the sealing force curve. Loss of contact directly leads to leakage and collision can lead to leakage because the shape of the seal jacket is likely to change permanently.

Finite element modeling

Mass scaling was needed to keep the analysis time reasonable. During the assembly steps 1) to 3), the scaling factor was not increased above 100 to avoid artificial inertial effects. During excitation a scaling factor of 400 was considered acceptable because as long as the seal lip stayed in contact with the counterface artificial inertial effects were not perceived. With these settings and a total analysis time of 2.2 s, the analysis was typically left to run overnight on a PC workstation.

The mesh density was chosen so as to adequately describe the overall dynamic behavior of the seal profile. For contact related phenomena, e.g. wear, mesh refinement in the seal lip region is needed to produce a more accurate contact pressure distribution. Submodeling of the contact region could therefore be considered. For condition monitoring purposes a model of reduced computational complexity would, however, be needed to provide fast enough feedback. Further work should involve assessment of changes in the contact situation over time due to, e.g., wear and creep.

CONCLUSIONS

The studied seal design could handle the measured axial displacements between the sealing surfaces without loss of contact. However, there is not much allowance for larger displacements. The seal housing needs to be designed to protect the seal against excessive compression causing irreversible deformation.

It appears that the current seal lip design does not represent a significant improvement over the earlier design as a contact pressure distribution similar to the previous one was produced. The current design can be further improved by increasing the dimensions of the cross-section to account for larger displacements.

Increased friction between spring and seal did not influence the axial dynamic behavior of the seal for the range of tested friction coefficient values (0.06–0.36).

The total seal-counterface contact force output from the finite element model could be used as a virtual force sensor to monitor and record the contact variations during operation.

REFERENCES

1. Calonius, O. and Pietola, M., Explicit Finite Element Analysis of Spring-Energized Rotary Face Seal for Industrial Process Machinery, 18th Abaqus Users' Conference, Stockholm, Sweden, 18-20 May 2005.
2. Hoffman, C., Untersuchungen an PTFE-Wellendichtungen, Dissertation, Universität Stuttgart, Institut für Maschinenelemente, Bericht Nr. 61, 1995.
3. Sui, H., Pohl H., Schomburg U., Upper U., and Heine S., Wear and Friction of PTFE Seals, Wear, 1999, **224**, pp. 175-182.
4. Pohl, H., Computerunterstützte und experimentelle Untersuchungen von Manschettendichtungen aus glasfaserverstärktem PTFE-Compound, Dissertation, Universität der Bundeswehr, Hamburg 1999.
5. MatWeb Online Materials Database: www.matweb.com, accessed 31.10.2003.
6. Abaqus Analysis User's Manual, Abaqus Inc., Providence, 2004, Ch. 7.16 Mass Scaling.
7. Kawahara, Y., Abe, M. and Hirabayashi, H., An Analysis of Sealing Characteristics of Oil Seals, ASLE Transactions, 1980, **23**, pp. 93-102.
8. Müller H.K., Concepts of Sealing Mechanism of Rubber Lip Type Rotary Shaft Seals, Proceedings of the 11th International Conference on Fluid Sealing, 1987, pp. 698-709.
9. Salant R.F., Theory of Lubrication of Elastomeric Rotary Shaft Seals, Journal of Engineering Tribology, 1999, **213**, pp. 189-201.